Functionality of wheat straw-derived biochar enhanced its efficiency for actively capping Cd and Pb in contaminated water and soil matrices: Insights through batch adsorption and flow-through experiments

Yasir Hamid, Yonglong Chen, Qiang Lin, Muhammad Haris Mahyuddin, Muhammad Usman Hadi, Muhammad Saqib Rashid, Ioannis Anastopoulos, Bilal Hussain, Hayssam M Ali, Fakhir Hannan, et al.

Journal Pre-proof

Functionality of wheat straw-derived biochar enhanced its efficiency for actively capping Cd and Pb in contaminated water and soil matrices: Insights through batch adsorption and flow-through experiments

Yasir Hamid, Yonglong Chen, Qiang Lin, Muhammad Haris, Muhammad Usman, Muhammad Saqib Rashid, Ioannis Anastopoulos, Bilal Hussain, Hayssam M. Ali, Fakhir Hannan, Xianyuan Yin, Xiaoe Yang

PII: S0045-6535(24)01664-3

DOI: https://doi.org/10.1016/j.chemosphere.2024.142770

Reference: CHEM 142770

To appear in: *ECSN*

Received Date: 2 April 2024

Revised Date: 20 June 2024

Accepted Date: 3 July 2024

Please cite this article as: Hamid, Y., Chen, Y., Lin, Q., Haris, M., Usman, M., Saqib Rashid, M., Anastopoulos, I., Hussain, B., Ali, H.M., Hannan, F., Yin, X., Yang, X., Functionality of wheat straw-derived biochar enhanced its efficiency for actively capping Cd and Pb in contaminated water and soil matrices: Insights through batch adsorption and flow-through experiments, *Chemosphere*, https://doi.org/10.1016/j.chemosphere.2024.142770.

Functionality of wheat straw-derived biochar enhanced its efficiency for actively capping Cd and Pb in contaminated water and soil matrices: Insights through batch adsorption and flow-through experiments

Yasir Hamid[1], Yonglong Chen[1], Qiang Lin[1], Muhammad Haris[2], Muhammad Usman[3], Muhammad Saqib Rashid[4], Ioannis Anastopoulos[5], Bilal Hussain[1], Hayssam M. Ali[6], Fakhir Hannan[7], Xianyuan Yin[8**], Xiaoe Yang[1*]

[1]Ministry of Education (MOE) Key Lab of Environ. Remediation and Ecol. Health, College of Environmental and Resource Sciences, Zhejiang University, Hangzhou 310058, China

[2]School of Environmental Science and Engineering, Shaanxi University of Science & Technology, Xi'an 710021, PR China

[3]Université de Rennes, Ecole Nationale Supérieure de Chimie de Rennes, CNRS, ISCR-UMR 6226, F-35000, Rennes, France

[4]Key Laboratory of Plant Nutrition and Fertilizer in South Region, Ministry of Agriculture, Guangdong Key Laboratory of Nutrient Cycling and Farmland Conservation, Institute of Agricultural Resources and Environment, Guangdong Academy of Agricultural Sciences, Guangzhou 510640, China

[5]Department of Agriculture, University of Ioannina, UoI Kostakii Campus, 47100 Arta, Greece

[6]Department of Botany and Microbiology, College of Science, King Saud University, Riyadh– 11451, Saudi Arabia

[7]Institute of Crop Science, Ministry of Agriculture and Rural Affairs Laboratory of Spectroscopy Sensing, Zhejiang University, Hangzhou, 310058, China

[8]Beautiful Village Construction Center of Quzhou Agriculture and Rural Affairs Bureau, Quzhou 324002, People's Republic of China

* **Corresponding author**: xeyang@zju.edu.cn (X. E Yang), 1121759696@qq.com (X. Yin)

Graphical abstract

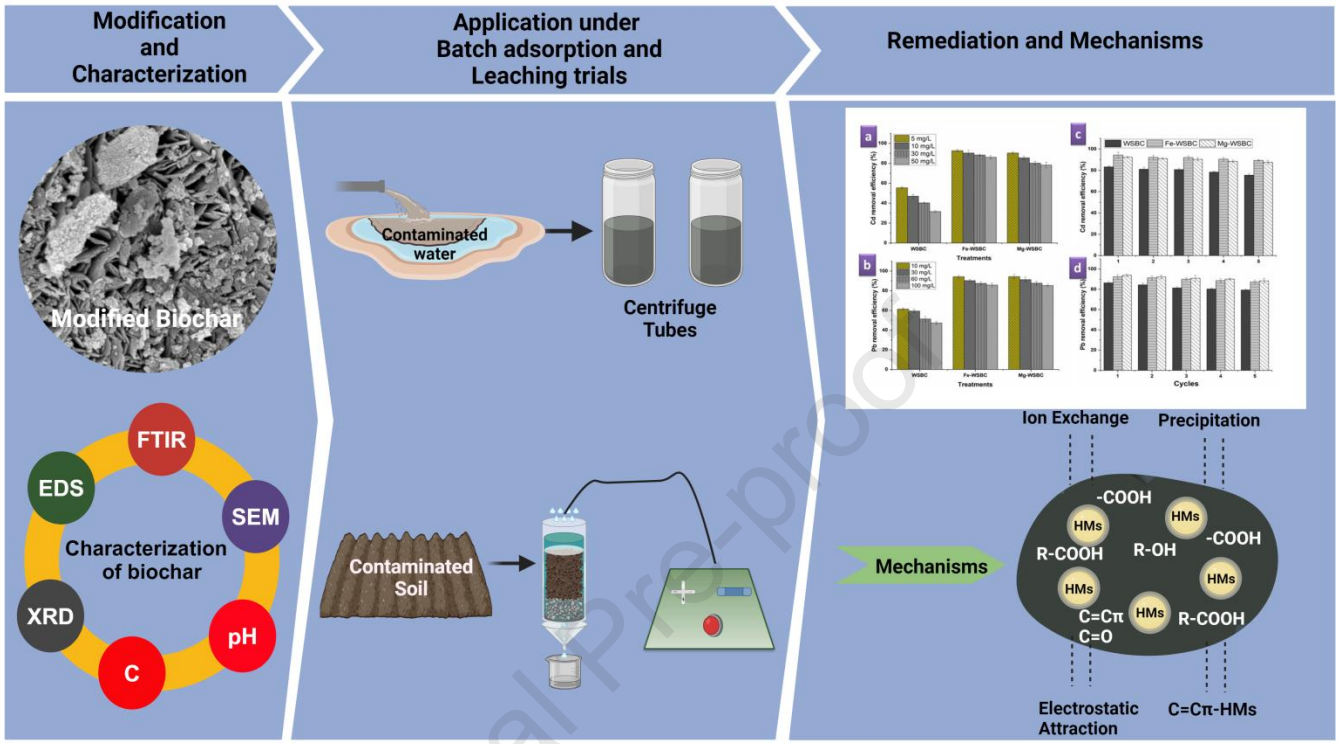

Functionality of wheat straw-derived biochar enhanced its efficiency for actively capping Cd and Pb in contaminated water and soil matrices: Insights through batch adsorption and flow-through experiments

Abstract

The impact of functionality of biochar on pressing environmental issue of cadmium (Cd) and lead (Pb) co-contamination in simultaneous soil and water systems has not sufficiently reported. This study investigated the impact of Fe- and Mg-functionalized wheat straw biochar (Fe-WSBC and Mg-WSBC) on Cd and Pb adsorption/immobilization through batch sorption and column leaching trials. Importantly, Fe-WSBC was more effective in adsorbing Cd and Pb (82.84 and 111.24 mg g^{-1}), regeneration ability (removal efficiency 94.32 and 92.365), and competitive ability under competing cations (83.15 and 84.36%) compared to other materials (WSBC and Mg-WSBC). The practical feasibility of Fe-WSBC for spiked river water verified the 92.57% removal of Cd and 85.73% for Pb in 50 mg L^{-1} and 100 mg L^{-1} contamination, respectively. Besides, the leaching of Cd and Pb with Fe-WSBC under flow-through conditions was lowered to (0.326 and 17.62 mg L^{-1}), respectively as compared to control (CK) (0.836 and 40.40 mg L^{-1}). In short, this study presents the applicable approach for simultaneous remediation of contaminated water and soil matrices, offering insights into environmentally friendly green remediation strategies for heavy metals co-contaminated matrices.

Keywords: Adsorption; Complexation; Functionalized biochar; Leaching; Soil; Water

1. Introduction

The rapid pace of industrialization has been recognized as a significant factor contributing to an alarming increase in ecological and human health problems, related to heavy metals. The contamination of soil and water environment with cadmium (Cd) and lead (Pb), has become a universal distress due to the lack of effective technologies capable of containing them within contaminated matrices (Habte et al., 2020). Adsorption/immobilization is a promising technique for removing heavy metals, due to its operational ease, cost effectiveness and simplistic design (Yu et al., 2021). However, success of this approach is highly influenced by several factors such as adsorption ability as well selectivity for contaminants (Hafeez et al., 2022). Therefore, it is essential to develop an economically viable and environmentally beneficial technique, capable of tackling the heavy metals contamination in different contaminated matrices e.g. soil and water system.

The success of the United Nations Sustainable Development Goals depends on several factors, such as safe utilization of agricultural wastes, sustainable management of contaminated soils and waters and ensuring a clean environment with safe food and water (Shaheen et al. 2022a, b). Since ancient times, straws have served various purposes, including fuel, animal feed, fertilizers, and basket making, however, a significant amount of straw is either wasted or burned (20% burned in field), with only a small portion being utilized in industries as raw material or for energy production (Ren et al., 2019). Therefore, it is of utmost preference to safely recycle the substantial quantities of straws in order to prepare affordable material for the remediation of contaminated matrices.

Biochar has garnered attention as a cost-effective, renewable and efficient adsorbent which is derived from various materials including plant straws, corncob, chicken litter, plant leaves, coconut shell, animal manure, and rice husk (Luo et al., 2019). Previously biochar has gained substantial attention for their application in improving soil fertility, crop productivity, increasing carbon stock in soil, pollutants remediation etc. (Haris et al., 2021). In general, pristine biochar contains a variety of functional groups

(Boni et al., 2020), however, its simultaneous application for multi contaminants under different environmental matrices is restricted due to inherent disadvantages, such as separation form aqueous solution and associated risks.

Alternatively, functionalized biochar has shown considerable potential to sequester the heavy metals by offering additional active sites (Cai et al., 2021). Therefore, in recent days, the development of cost effective, efficient, environmental friendly and stable biochar adsorbents has gained attention for the remediation of contaminated matrices (Hamid et al., 2022). However, most of the fabrication approaches involves the complicated procedures as well multi-steps, including co-precipitation, pyrolysis, and functionalization, thus making the synthesis of functionalized biochar difficult and expensive. Hence, chemical precipitation or impregnation has become a cost-effective and eco-friendly method for the one-step production and functionalization of biochar, offering a broad range of applications (Jia et al., 2019; Wan et al., 2020). For instance, the adsorption capacity of magnetic biochar was demonstrated to 817.64 mg g^{-1} due to increased alkalinity of modified biochar (Dong et al., 2022). Similarly, the utilization of Mg-fabricated corncob biochar depicted a significant enhancement of Cd and Pb adsorption from wastewater by 2.36 and 9.34 times than simple biochar (Deng et al., 2021). To date, however, only a limited research have specifically investigated the simultaneous removal of heavy metals from water through batch adsorption experiments, as well their immobilization in soil profile using flow-through experiments, involving Fe and Mg-modified biochars. Moreover, it is essential to compare the efficacy of modified biochars for different heavy metals across diverse environmental settings to develop a cost-effective and environmentally sustainable adsorbent that can refine Cd and Pb contaminated matrices.

Herein, we proposed a one-step sustainable approach to modify wheat straw-derived biochar and produce Fe and Mg-modified biochar, by employing batch adsorption experiments for Cd and Pb under contaminated water, real river water, and acidic leaching conditions. Therefore, the synthesized biochar was utilized and evaluated for Cd and Pb abatement in water and soil matrix through various tests including adsorption, kinetics, pH, selectivity, real scale river water, and flow-through experiments. The

study also focused on elucidating the influence of modified biochars on selectively adsorbing Cd and Pb from a multi-cationic solution. In addition, the mechanisms for Cd and Pb removal were elucidated using state-of-the-art techniques e.g. EDS, XPS and XRD. Additionally, we conducted the study about relative leaching of contaminants from the contaminated soil with the use of pristine and modified biochars. The study was designed to achieve these objectives (1) clarifying the adsorptive ability of functionalized biochar for the removal of Cd and Pb from co-contaminated soil and water, (2) investigating the mechanisms of functionalized biochar for the removal of Cd and Pb by deploying innovative techniques, and (3) elucidating the impact of functionalized biochar on Cd and Pb leachability under acidic conditions.

2. Materials and methods

2.1. Materials

The entire chemical stock was either analytical grade or advanced grade and was consumed without modification. The $CdCl_2$ (99%) and $PbCl_2$ (AR grade) were derived by Aladdin, China, and were utilized to prepare stock solution with ultra-pure water (18.2 MΩ.cm at 25 °C). While, $FeCl_3$ (99%), $FeSO_4 \cdot 7H_2O$ (99%), $MgCl_2.6H_2O$ (99%), HCl and NaOH (>96%) were developed by Sinopharm Chemical Reagent Co., Ltd (Shanghai, China). pH of the solution was adjusted using 0.1 M HNO_3 or 0.1 M NaOH and measured with a pH meter (PB-10, Sartorius, Germany). Cd and Pb concentration was determined using ICP-MS (inductively coupled plasma mass spectrometry) (Agilent, 7500a, USA).

2.2. Preparation and characterization of simple and modified wheat straw biochar

Wheat straw biochar (WSBC) was prepared by collecting straw from an agricultural farm located in Shangyu county, Shaoxing city, Zhejiang, China (30° 01′ 00″ N, 120° 52′ 00″ E). The straws were air dried, chopped into small pieces and subjected to biochar production at 700 ^oC under oxygen deficient

conditions for 1.5 h. The wheat straw biochar (WSBC) was further impregnated with Fe and Mg oxides to elevate the diversity of functional groups onto biochar. In short, WSBC (50 g) produced at 700 ^{o}C was suspended in distilled water (500 mL) and magnetized with Fe by mixing solutions of $FeCl_3$ and $FeSO_4 \cdot 7H_2O$ (18 g in 1.3 L water and 36.6 g in 150 mL water separately), respectively. Both solutions were vigorously mixed while constantly stirring for 5 min at 200 rpm (60-70 ^{o}C). Following that, the mixed solution (Fe^{2+}/Fe^{3+}) was softly poured in other beaker containing suspended biochar (50 g) by continuous stirring for 30 min at 50 rpm (room temperature). Finally, the pH of biochar containing solution was maintained at ~10–11 by adding 10 M NaOH, filtered and repetitively washed with purified water and ethanol. The residual blend was dried out in an oven (50 ^{o}C) and resulting biochar was termed as Fe-WSBC.

Furthermore, 10 g WSBC was agitated with 1 M solution of $MgCl_2.6H_2O$ (100 mL) for 2 h. The mixture underwent washing for a number of periods with deionized water and oven-dried for 24 h at 70 ^{o}C. The modified biochar was termed as Mg-WSBC.

Biochars were comprehensively characterized using innovative techniques e.g. SEM (Gemini SEM 300, Germany), FTIR (Nicolet 6700 spectrometer), EDS (EDAX Inc. Genesis XM), XRD (Bruker D8 Advance) and XPS. Additionally, pH was noted with a pH meter, while elemental ratio (C, H, and N) was determined using an elemental analyzer (varioMICRO CHN). The basic physicochemical properties of all biochars are presented in Table S1.

2.3. Batch adsorption studies

Batch adsorption experiments were conducted using Cd and Pb stock solutions (1000 mg L^{-1}), prepared by ultrapure water. Cd and Pb concentrations (10, 20, 30, 50, 80, 100, 150, 200, 250, 300 mg L^{-1}) were established by constantly diluting the corresponding stock solution.

2.3.1. Kinetic studies

The kinetic adsorption experiment for single metal solution involved the addition of 0.02 g of each type of biochar (WSBC, Fe-WSBC and Mg-WSBC) to 30 mg L^{-1} Cd or Pb solution (40 mL). The experiment was conducted in a water bath shaker (200 rpm, 26 ± 2 °C) by maintaining solution pH at 6 ± 0.5. The triplicate samples were collected at defined intervals (5, 10, 20, 30, 60, 120, 240, 480, 960, and 1440 min). The samples were then centrifuged for 10 min, filtered using 0.22 µm membrane filters for Cd and Pb concentrations using ICP-MS. The adsorbed amount of Cd and Pb and their respective removal percentage from the solution was calculated with following equations:

$$Qe = \frac{(Co-Ce)*V}{m} \quad (1)$$

$$R\% = \frac{(Co-Ce)}{Co} * 100 \quad (2)$$

Where, Qe is the adsorptive ability of biochar for Cd and Pb, while R defines the removal percentage; primary concentration (mg L^{-1}) of Cd and Pb is portrayed by Co; Ce depicts the equilibrium concentration of Cd and Pb (mg L^{-1}); V (L) and m (g) stand for solution volume and biochar mass, respectively.

Moreover, the quantitative description about the adsorption of Cd and Pb onto biochar was measured through pseudo first order (PFO) and pseudo second order (PSO) models (Boparai et al., 2011).

The intraparticle diffusion model (IPD) examines the adsorption kinetics and diffusion mechanisms of Cd and Pb onto WSBC, Fe-WSBC and Mg-WSBC (Zhou et al., 2017).

PFO $$Q_t = Q_e\left(1 - e^{(-k_1 t)}\right) \quad (3)$$

PSO $$Q_t = \frac{k_2 Q_e^2 t}{1+k_2 Q_e t} \quad (4)$$

IPD $$Q_t = k_i t^{0.5} + C \quad (5)$$

Where, Q_t and Q_e represent the adsorbed amount of Cd and Pb (mg g^{-1}) at time (t) and equilibrium, respectively; k_1 (1 min^{-1}) and k_2 (g mg^{-1} min^{-1}) are kinetic rate constant of PFO and PSO; k_i is the intraparticle diffusion rate constant; the boundary layer thickness (mg g^{-1}) is denoted by C. Nonlinear

regression calculated the parameters of PFO and PSO. The details regarding adsorption isotherm experiments and effect of solution pH are presented in Supplementary materials data section S1 and S2.

2.3.2. Selectivity and regeneration trials

The selective adsorption of Cd and Pb with WSBC, Fe-WSBC and Mg-WSBC was investigated by adding 0.02 g of adsorbents into a mixture of solution containing Cd, Pb, Cu, Zn and Ni. The solutions were put in 50 mL centrifuge tubes with pH 6 ± 0.5, 24 h agitation at 200 rpm and 25 ± 1 ^{o}C temperature. The contents of Cd and Pb in the supernatant were analyzed using ICP-MS.

The regeneration trial for Cd or Pb adsorption was conducted by reacting the WSBC, Fe-WSBC and Mg-WSBC with 2 mL of HCl/HNO_3 for 1 h at 25 ± 1 ^{o}C and 200 rpm. The regeneration experiments of all the adsorbents were conducted for a minimum of five times to understand their efficiency for metals removal for extended experiments and value was noted using ICP-MS.

2.3.3. Real sample application of WSBC, Fe-WSBC and Mg-WSBC

The real scale efficiency of WSBC, Fe-WSBC and Mg-WSBC was assessed by using real river water (Zhixi River, pH 7.59), Quzhou city and Zhejiang province which was further spiked with Cd or Pb to gain better understanding of the real scale application of produced additives. Briefly, collected river water was spiked with four different concentrations of Cd (5, 10, 30, and 50 mg L^{-1}) and Pb (10, 30, 60, and 100 mg L^{-1}). Later, the adsorbents (0.02 g) was separately loaded into 40 mL of spiked river water and agitated for 24 h at 200 rpm and subjected to ICP-MS for residual fraction measurements.

2.4. Flow-through experiments

Column leaching trials were initiated by thoroughly mixing the WSBC, Fe-WSBC and Mg-WSBC (2%) with a multi-contaminated soil from Shangyu County. The soil contained variable levels of metals, including Cd (10.30 mg kg^{-1}), Pb (230.39 mg kg^{-1}), and Cr (65.08 mg kg^{-1}) that was collected. A blank column containing only soil (CK) was introduced for comparison. Subsequently, amended and non-

amended soil (400 g) was placed in 30 cm X 5 cm (L/W) PVC pipes, making three replicates for each treatment. Before filling the columns with soil, the column base was fixed with a filter paper and stuffed with impurities free quartz sand (1 M HCl washing). Top of the column was also packed with quartz sand to facilitate water flow and to avoid soil-water direct contact. Throughout the experiment, the columns were supplied with a steady flow of acidic water solution (pH 4.5: to meet the composition of typical acid rain of Yangtze River Delta) at 1.73 mL/min. Leachates were collected at intervals of 1, 3, 7, 14, and 21 days by passing 100 mL of acidic solution at each leaching time. Variations in leachate pH and EC with applied additives was measured immediately, while the leachable heavy metals concentration was determined by passing the collected leachate through a 0.22 μm filter membrane (Jinteng Tianjin, China). The detailed information regarding Cd and Pb availability and fractions in soil is presented in Supplementary materials data section S3.

2.5. Data analysis and quality parameters

The biochars were prepared by following the standard methods as outlined in section 2.2. Batch adsorption and column leaching tests were performed with three replicates. Prior to use different consumable such as, PVC pipes, centrifuge tubes, and glassware were washed with 10% HNO_3 acidic solution followed by distilled water. All the existing data represent means of three replications ± S.E (standard error). Treatment means were differentiated with one-way ANOVA, Duncan's test, and statistical software SPSS 20.0. Graphical illustrations were generated using Origin 2022.

3. Results and discussion

3.1. Characteristics of WSBC, Fe-WSBC and Mg-WSBC

The elemental composition of simple and modified biochars is presented in Table S1. The elemental analyzer results indicated a reduction in C and N content of Fe-WSBC and Mg-WSBC, while indicating

the increased H contents in Mg-WSBC (3.68%) compared to WSBC (1.21%). Moreover, the atomic ratios such as H/C and C/N, offers valuable information about the aromatic characteristics, polarization and hydrophobicity of adsorbents (Xu, J et al., 2022). The results revealed a reduction in C/N ratio and increased H/C ratio after the modification as evidenced by the values of 0.139 and 0.037 for Mg-WSBC and Fe-WSBC, respectively. The Fe and Mg contents of modified biochar were measured through EDS analysis which depicted that modification also resulted in higher Fe and Mg contents in Fe-WSBC (24.37% Fe) and Mg-WSBC (30.10% Mg), which were low in WSBC (0.61 and 4.31%, respectively), indicating the successful loading of Fe and Mg onto modified biochars.

The SEM images clearly showed the distinct morphological differences between pristine and modified biochars, where WSBC presented irregular tiny patches with smooth surface (Figure S1). In contrast, Fe-WSBC depicted a more porous and heterogeneous structure, which could potentially improve the adsorption of metals. In addition, Mg-WSBC showed columnar crystal appearance, offering additional adsorption sites. This modification ultimately contributed in the destruction of the carbon skeleton in Mg-WSBC, converting the structure into agglomerated blocks, thereby providing more adsorption sites for Cd and Pb.

The various spectra of FTIR illustrated the changes in functional properties of biochar (Figure S1). The band strength at 3422 cm^{-1} indicated the existence of (-OH), while other peaks at 1560 cm^{-1} were assigned to -CH2-. Moreover, the thermal degradation of lignin and cellulose causes biochar to develop aliphatic, ester and aromatic functional groups. Modification with Fe indicated wider carboxyl group and alcoholic functional groups (–OH groups) at 3415 and 1560 cm^{-1} (Kristianto et al., 2016; Godlewska et al., 2020). Meanwhile, distinctive stretching bands at 1637 and 1618 cm^{-1} manifested the presence of carbonyl group. A decrease in intensity from 1116 to 1637 cm^{-1} might be allied to the aromatic ring decomposition or due to the stretches in –OH group and C–O in hydroxyls (Li, B et al., 2017). A new and strong peak at 3406 cm^{-1} indicated the broadening vibration of –OH, confirming the $Mg(OH)_2$ abundance in Mg-WSBC, indicating the successful loading of Mg onto biochar. Moreover, sharp and broadening

peaks associated with carboxylic groups and aromatic structures (C=O) were detected at 1630 cm^{-1} and 1033 cm^{-1}, respectively (Deng et al., 2021). The wide vibrations at 606 cm^{-1} indicated the presence of Mg-O in Mg-WSBC (Tan et al., 2019). Moreover, the peak height ratio of Fe-WSBC and Mg-WSBC increased compared to WSBC, suggesting changes induced with the impregnation of certain materials.

The XRD analysis provided the information about crystal structure of simple and modified biochars (Figure S1). The presence of hollow peaks in biochar is indicated of amorphous structure, whereas well developed peaks designate the crystalline nature (Sackey et al., 2021). Therefore, in this study, WSBC exhibited the hollow or small peaks with low intensities, presenting its amorphous structure (2θ at 20–30°). Moreover, presence of sharp peak at 2θ= 26.76° indicated the existence of SiO_2 crystals (Naeem et al., 2019). However, the development of sharp crystal peaks in Fe and Mg modified biochar indicated the improved crystallinity of modified biochars. There was clear difference in peaks intensity of Fe-WSBC and Mg-WSBC where, corresponding deep peaks at 26.61 and 28.60° indicate the presence of Fe in FeOOH and Fe_2O_3, respectively (Zhang et al., 2016). Moreover, certain other peaks of lower intensities matched the diffraction patterns of Fe_2O_3 and Fe_3O_4 (Karunanayake et al., 2017). Similarly, well-defined crystal phases were observed in Mg-WSBC on various diffraction peaks. The sharp and large diffraction peak of 2θ=23.92°, 25.42°, 26.50°, and 28.26° indicated the abundance of $Mg(OH)_2$. Moreover, spectral vibrations at 2θ values of 36.38° and 40.42° indicated the presence of MgO (Zhang et al., 2012). Therefore, the presence of these elements onto modified biochars confirms the crystallinity of Fe-WSBC and Mg-WSBC (Zheng et al., 2020).

3.2. Batch adsorption studies

3.2.1. Adsorption kinetics of Cd and Pb

Adsorption kinetic experiments are important for identifying the rate-limiting factors and understanding the mechanisms governing the mass transfer of pollutants. Figure 1 depicted the evaluation of the adsorption potential of WSBC, Fe-WSBC and Mg-WSBC for Cd and Pb using PFO, PSO and IPD

models. The adsorption of Pb demonstrated a gradual increase with extended contact time, eventually reaching a stabilized state after certain time period (Boni et al., 2020). The adsorption process is mainly divided into three phases: initial rapid adsorption, followed by slower increment in adsorption and finally equilibrium adsorption. The rapid initial adsorption of metallic cations may be attributed to the abundance of un-occupied adsorptive sites (Ma, Y et al., 2021). Among the tested adsorbents, as presented in Figure 1, Fe-WSBC had the maximum adsorption capacity for Cd and Pb, followed by Mg-WSBC and WSBC (22.38, 16.45, 8.44; 35.25, 28.34, 15.45 mg L^{-1}), respectively. The adsorption of Cd and Pb reached to maximum within 0-60 minutes and become stabilized between 120-150 minutes of reaction. The rapid adsorption followed by slower removal is consistent with the results of Song et al. (2021), who reported similar trend for Pb removal using a composite of sewage sludge biochar and chitosan composite. Furthermore, the R^2 value for PSO approached to 1 as indicated in Table S2. These results showed that chemisorption as regulatory mechanism for the adsorption of Cd and Pb (Haris et al., 2023; Haris et al., 2024). Based on the adsorption kinetic curves (Figure 1) it can be shown that modified biochar reaches equilibrium within 60 min, indicating fast adsorption event. Moreover, the k constant also works as time-scaling element and governs the rate at which equilibrium is reached (Haris et al., 2022). Consequently, PSO model was used to extrapolate the k values which evaluated the adsorption rate and indicates the higher k value of Fe-WSBC, exhibiting short equilibrium time.

The intraparticle diffusion model mainly comprehends the adsorption mechanism, specifically the contribution of internal diffusion throughout the adsorption method. The plot of Q_t vs $t^{0.5}$ for Cd and Pb adsorption onto WSBC, Fe-WSBC and Mg-WSBC presented three distinct slopes displaying the external diffusion, intraparticle diffusion, and final equilibrium diffusion (Figure 1) (Table S3). The graphs for all biochar samples have a linear relationship that passes through the origin, signifying that adsorption is governed by the intraparticle diffusion. The values of IPD contstants for WSBC, Fe-

WSBC and Mg-WSBC presented a decline in the order of kp1 > kp2 > kp3, pointing the involvement of internal diffusion during the adsorption process (Haris et al., 2022; Haris et al., 2023). The IPD constant (k_p) values decreased in subsequent order $k_{p1} > k_{p2} > k_{p3}$, confirming the internal diffusion as a sorption process (Haris et al., 2022; Haris et al., 2023), where k_p values for Fe-WSBC were higher (1.53, 0.147, 0.043 and 4.10, 0.123, 0.038) than WSBC (0.36, 0.08, 0009 and 1.66, 0.109, 0.009), respectively for Cd and Pb (Table S3). These results further clarify the faster adsorption diffusion in Fe-WSBC, correlating with the findings of PSO.

3.2.2. Adsorption isotherms

The adsorption isotherm is the interface between the amount of adsorbate (q_e) being uptaken by the adsorbent as well the adsorbate (C_e) concentration when equilibrium is achieved (Haris et al., 2021). The adsorption isotherms of Cd and Pb onto simple and modified biochars are presented in Figure 1 and Table 1. Cd and Pb adsorption capacity for all the biochars decreased by following trend: Fe-WSBC > Mg-WSBC > WSBC (82.8 > 65.4 > 34.2 mg g^{-1}) and (111.24 > 88.64 > 48.2 mg g^{-1}), respectively. The elevated Pb adsorption might be attributed to its stronger electronegativity compared to Cd as well the smaller hydrated radii of Pb than Cd in the solution. Fe-WSBC showed higher adsorption which was substantially higher compared to other biochars, indicating its potential for effectively adsorbing Cd and Pb from contaminated matrices. Langmuir model better described the adsorption of Cd and Pb onto WSBC, Fe-WSBC and Mg-WSBC with corresponding R^2 values of 0.981, 0.982, 0.992 and 0.993, 0.991, 0.990, respectively, depicting the monolayer adsorption onto modified biochars. On the opposing, Freundlich and Temkin isotherm models, also explained the adsorption behavior of biochars for Cd and Pb (R^2: 0.970, 0.966, 0.959; 0.911, 0.899, 0.932) and (R^2: 0.989, 0.979, 0.986: 0.911, 0.931, 0.948), respectively, however, Langmuir model was more precise in relating the adsorption isotherm (R^2: 0.981, 0.982, 0.992: 0.993, 0.991, 0.990), presenting the monolayer adsorption by identical surfaces and limited sites (Tehrani et al., 2017). The increase in maximum adsorption capacity can be attributed to the porosity

and the active Fe and Mg functional groups of the modified biochar. Hence, the usage of Fe-WSBC have shown superior efficacy for Cd and Pb removal as compared to other biochars. These results suggest that Fe-WSBC could be a promising tool for the long-term application in curbing Cd and Pb removal from aqueous mediumSimilar results about the Cd and Cu adsorption with modified and simple biochar were reported by Wang et al. (2019) and Xiao et al. (2020), emphasizing the high affinity of functional groups on the biochar surface for metals adsorption.

3.2.3. Effect of solution pH

The solution pH significantly influences the Cd and Pb adsorption by inducing chemical speciation in water and the availability of active sites on the adsorbents. The adsorption of Cd and Pb with WSBC, Fe-WSBC and Mg-WSBC treatment in a single adsorption system was carried out with initial pH range of 3-10 and removal efficiency is presented in (Figure S3). The results revealed that increasing the pH from 3-6 notably enhanced the Cd removal from 46.35 to 85.67%, 51.02 to 91.36%, and 52.18 to 90.57% with WSBC, Fe-WSBC and Mg-WSBC treatment, respectively. Similarly, elevating the pH from 3 to 7 led to improved Pb removal by 84.36, 90.06, and 89.63% with WSBC, Fe-WSBC and Mg-WSBC application, respectively. This elevated Cd and Pb removal with a change in pH might be attributed to the reduced electrostatic repulsion between heavy metals and adsorbents (Lun et al., 2019). At lower pH value, the adsorbents were protonated which impeded the heavy metals removal from solution via electrostatic attraction (Tie et al., 2023). Moreover, protonation of functional groups also contributed to electrostatic repulsion among the active sites, resulting in lower Cd and Pb removal from contaminated solution (Tumampos et al., 2021). The biochars demonstrated a higher capacity for Cd and Pb removal in solution with a pH range of 6.0, which further confirms the potential use of single step modification of biochar in effectively curbing the Cd and Pb from contaminated waters. This effective adsorption of biochar is attributed to the strong attraction of modified biochar with heavy metals through electrostatic forces in aqueous system.

3.2.4. Influence of ionic strength

Industrial wastes often contains a mixture of metal cations, including Zn^{2+}, Ni^{2+} and Cu^{2+}, which can hinder the removal of some specific cations due to competing adsorption (Haris et al., 2023). Thereby, an investigation about the competitive ability of Cd and Pb with Cu, Zn and Ni for adsorptive sites on WSBC, Fe-WSBC and Mg-WSBC was conducted by employing adsorption experiment (pH 6 ± 0.5, agitated for 24 h at 200 rpm (25 ± 1 ^{o}C)). As shown in Figure S4, the effect of metal cations and their concentration showed variable difference, with high concentration of competing cations inhibiting the Cd and Pb contents. Moreover, low concentration of Cu, Ni, and Zn (20 mg L^{-1}) also inhibited the Cd and Pb adsorption which was highly retarded at 100 mg L^{-1} of competing cations. However, among the three biochars, Fe-WSBC demonstrated higher effectiveness in removing Cd from multi-contaminated solution even with higher concentration of competing cations, achieving 83.15 and 80.19% removal with increasing Zn and Ni concentration (100 mg L^{-1}), respectively. Moreover, Fe-WSBC and Mg-WSBC resulted in greater levels of Pb retention, revealing 84.36, 80.47, 80.14% and 85.45, 84.39, 79.65% removal at 100 mg L^{-1} of Cu, Zn and Ni, respectively. The above results indicate the strong affinity of Cd and Pb to modified biochars (Deng et al., 2021). The higher adsorption of Cd and Pb with Fe-WSBC and Mg-WSBC as compared to WSBC, even at elevated levels of competing cations, suggests that adsorption sites were completely captured by Cd and Pb through complex formation (Xiao et al., 2018). In a recent study, Ke et al. (2022) also reported the preferred adsorption of Cd from a Cd/Zn binary adsorption system. These findings explain the potential use of modified biochars for Cd and Pb removal in real wastewater systems.

3.2.5. Adsorption mechanisms

The identification of adsorption mechanisms is crucial to understand the environmental fate of heavy metals and the practical application/utilization of prepared adsorbents (Figure 6). Adsorption of toxic substances onto modified biochars involves numerous mechanisms e.g. physical adsorption, precipitation,

and ion-exchange (Jin et al., 2016). Therefore, FTIR and XRD analysis were employed to further explore the mechanisms of Cd and Pb adsorption onto WSBC, Fe-WSBC and Mg-WSBC (Figure 2a,b,c).

The physical changes that occure after modification is determined by the functional moieties of biochar. For this purpose, FTIR spectroscopy was employed to investigate the adsorption of Cd and Pb onto biochars (Figure 2). The change in FTIR spectrum after Cd and Pb adsorption onto Fe-WSBC and Mg-WSBC indicates the formation of new functional groups and modification of existing ones. The new peaks observed for Fe-WSBC and Mg-WSBC at 617 and 604 cm^{-1} might be assigned to the development of Pb precipitates ($PbCO_3$) (Cao et al., 2019). Moreover, the shifting of bands from 1560 cm^{-1} to 1618-1632 cm^{-1} indicates Cd/Pb interaction with π-electron (Cai et al., 2021). Notably, Fe-WSBC exhibited a decrease in the intensity of OH stretching vibration peak, signifying the consumption of hydroxyl groups during the adsorption process (Chen et al., 2017). This could be due to the interaction of hydroxyl groups with the Cd and Pb, resulting in the formation of metal-hydroxyl complexes. Meanwhile, new peaks between 400-700 cm^{-1} were assigned to the formation of metal-oxygen bonds, while the shifting of stronger peak at 1637 cm^{-1} to a lower wavenumber identifies the COO–M complexes. This suggests the interaction of carboxylate groups present in Fe-modified biochar with the heavy metal ions, resulting in the displacement of the H^+ ion and formation of metal-carboxylate bond (Zhou et al., 2018).

On the other hand, FTIR spectra of Mg-WSBC after Cd and Pb adsorption also showcased the changes in peaks corresponding to the carbonyl (-C=O) group, which shifted to a higher frequency, indicating the formation of complexes with Cd and Pb (Novak et al., 2010). Furthermore, the carboxyl (-COOH) group, responsible for the acidic properties of Mg-WSBC, also undergoes changes in the FTIR spectra after Cd and Pb adsorption (Wang et al., 2013). The peak corresponding to the carboxyl group shifted to a lower frequency, indicating the complexation mechanisms of Cd and Pb with this functional group. Overall, the changes in peak intensities after Cd and Pb adsorption onto Fe-WSBC and Mg-WSBC involve several mechanisms, including electrostatic interaction and complexation (Ni et al., 2019).

Figure 2 displays the XRD spectra of WSBC, Fe-WSBC and Mg-WSBC after Cd and Pb adsorption. When applied to biochar samples, XRD can provide information about the mineral composition and crystalline structure of the material after heavy metals adsorption from contaminated matrices (Kang et al., 2022). In this case, XRD spectra of modified-wheat straw biochar after Cd and Pb adsorption can reveal insights into the interactions between biochar and the contaminants. The XRD spectra of Fe-WSBC and Mg-WSBC after Cd and Pb adsorption indicated the variation in peak strength that were designated to the presence of $CaCO_3$, indicating the dissolution or transformation after Cd or Pb adsorption (Eom et al., 2022). Moreover, a lower peak intensity of Fe_2O_3 and MgO revealed that these oxides were consumed throughout the adsorption process (Tao et al., 2019). The appearance of new diffraction peaks of Fe-WSBC and Mg-WSBC after Cd and Pb adsorption at 2θ, approximately between 25-35° might be related to presence of Cd or Pb-hydroxide particles. Overall, the XRD spectra of Fe-WSBC and Mg-WSBC after Cd and Pb adsorption provided valuable information about the mineral composition, crystalline structure and adsorption mechanisms with modified biochars, further demonstrating the potential of modified biochars as effective remediation tools in contaminated matrices.

The XPS spectral analysis can further demonstrate the adsorption mechanisms onto simple and modified biochars. Figure S2 presents the XPS spectral analysis of WSBC, Fe-WSBC and Mg-WSBC after Cd and Pb adsorption. After Cd adsorption onto Fe-WSBC, the Cd3d peaks at 405.35 eV and 411.58 eV indicated the adsorption of Cd onto modified biochar with specific Cd–O and $CdCO_3$ elements (Figure S2) (Li et al., 2016; Tang et al., 2020). Moreover, the FWHM (full width at half maximum) calculated the atomic percentage of each chemical bond and indicated that these bonds present 15% and 100%, respectively. Moreover, after Pb adsorption onto modified biochar, specifically Fe-WSBC, the peaks at 137.76 eV and 146.72 eV were attributed to Pb bonding (33%) (Gao et al., 2019). Overall, these results indicate that surface complexation and precipitation were mainly involved in Cd and Pb adsorption from contaminated water matrix (Wang et al., 2022; Sha et al., 2023).

3.2.6. Reusability of WSBC, Fe-WSBC and Mg-WSBC

The regeneration of adsorbents is a crucial to determine their efficacy and potential for reuse in contaminated environments. More precisely and specifically, modified biochar can be easily separated from contaminated aquesous solution by using centrifugation process following each adsorption-desorption test. The results revealed a notable decline in Cd and Pb removal over five cycles with WSBC, indicating a decrease of 83.24 to 75.47% and 86.41 to 79.36% after 5 cycles, respectively (Figure 3). However, Fe-WSBC demonstrated remarkable stability, maintaining Cd removal at 94.32 to 89.37% and Pb removal at 92.36 to 87.39% after 5 cycles. Meanwhile, Mg-WSBC indicated a minimum Cd and Pb removal efficiency of 87.49 and 88.35%, respectively, displaying a clear difference with pristine biochar (WSBC). This higher removal efficiency might be attributed to the abundant functional moieties (carboxyl, aromatic, and alcoholic) after biochar modification. It could be extrapolated that the modification of biochar showed excellent reusability, allowing them to be used for long time in practical applications.

3.2.7. Application of WSBC, Fe-WSBC and Mg-WSBC in river water

After 24 h of contact time, Fe-WSBC presented the highest removal of Cd (92.57%) in 5 mg L^{-1} Cd spiked water and 85.95% from 50 mg L^{-1} Cd spiked water (Figure 3). Moreover, Fe-WSBC and Mg-WSBC removed 85.73 and 85.24% of Pb from highest contaminated samples (100 mg L^{-1}). Despite the increased levels of heavy metals, Fe-WSBC and Mg-WSBC experienced higher removal efficiency, indicating the significant potential of modified biochars for practical application of water treatment in multi-contaminated matrices. The comparison of prepared adsorbents for this study with other already reported materials is presented in Table 2.

3.3. Flow-through experiment

3.3.1. Effect on leachate pH and EC

The pH of leachate displayed various patterns at different time intervals, showing notable differences among the amendments (Figure S5). The highest leachate pH was recorded during 5th leaching interval in columns treated with Mg-WSBC, presenting 2.11 unit difference with CK, followed by Fe-WSBC and WSBC (1.39 and 0.99 units higher), respectively. All the amendments gradually increased the leachate pH till last leaching cycle, presenting the following trend: Mg-WSBC > Fe-WSBC > WSBC > CK (7.50 > 6.73 > 6.38 > 5.39).

The inclusion of Fe-WSBC in the soil columns improved the EC value (2833 μS m^{-1}), in contrast to a sharp decrease observed in CK (1309 to 720 μS m^{-1}). Leachate from both Fe-WSBC and Mg-WSBC treated columns depicted similar trend of highest and lowest EC, with values 2833-160 μS m^{-1} and 2644-142 μS m^{-1}, respectively. This overall trend might be attributed to the buffering capacity of soil (Wang et al., 2019). The higher pH values with applied additives might be associated with alkaline nature, carbon mineralization and hydroxyl group production by ligand exchange (Van Poucke et al., 2020). However, the decline in leachate EC indicates the leaching of soluble ions (Page et al., 2014).

3.3.2. Effect on Cd and Pb contents of leachate

The addition of WSBC, Fe-WSBC, and Mg-WSBC to column soil led to a reduction in Cd and Pb concentrations in the leachate (Figure 4). It was found that Fe-WSBC effectively reduced the Cd content in leachate (to 0.326 mg L^{-1}) as compared to CK (0.835 mg L^{-1}). However, Mg-WSBC was more effective in reducing Pb contents (to 16.192 mg L^{-1}) followed by Fe-WSBC (17.628 mg L^{-1}), with no obvious difference between each other. Cd and Pb concentration was highest in CK following all leaching intervals, reaching values of 0.835 and 404.403 mg L^{-1}, respectively. Overall, these findings indicate the potential of biochar addition, particularly modified biochars, in effectively reducing the heavy metals content in leachate and providing a promising strategy for mitigating heavy metals pollution in soils (Fahmi et al., 2018). However, in this study, the high contents of Cd and Pb in leachate even with applied treatments might be related to short experimental time or specific leaching intervals. Previous studies

have reported that biochar owns the ability to adsorb heavy metals and prevent their leaching into the groundwater due to its high affinity for heavy metals retention in soil (Boni et al., 2020; Godlewska et al., 2020). Moreover, Fe and Mg-modified biochar holds improved properties such as increased surface area and pH, thereby enhancing the adsorption of heavy metals (Li, H et al., 2021a). Modified biochar also acts as a metal chelator, thus forming strong bonds with Cd and Pb. Similarly, Fe and Mg serve as a competitive ion, reducing the solubility of metals and reducing their leaching into the groundwater (Li, H et al., 2021a: Chen et al., 2022; Xu, J et al., 2022).

3.3.3. Effect on metals availability and fractionation in soil

Modified biochar has been proposed as potential amendment to diminish the heavy metals bioavailability in contaminated soils. Here, the potential of pristine and modified biochars was explored to mitigate the availability of heavy metals in soil after column leaching experiment (Figure 5). The results showed a considerable drop in available Cd and Pb in soil after leaching, which led to a significant reduction to 2.27 and 18.43 mg kg^{-1} in Fe-WSBC treated columns, respectively. Meanwhile, Mg-WSBC was also effective in lowering the Cd and Pb concentration to 2.48 and 21.43 mg kg^{-1}, respectively as compared to CK (4.45 and 46.75 mg kg^{-1}, respectively). It is important to note that the effectiveness of modified biochars in reducing the bioavailable heavy metals relies on pyrolysis temperature, type and amount of precursor used, and the type of biochar feedstock. Higher pyrolysis temperatures lead to the formation of more stable and recalcitrant biochars with enhanced sorption ability (Lei et al., 2019: Hamid et al., 2020). Prior studies reported that biochar produced from feedstock high in lignin and cellulose depicted greater sorption capacity compared to biochars produced from feedstock with high ash content. Moreover, the increased surface area and improved pore volume of impregnated biochar contribute to higher metal removal efficiency of biochar (Liu et al., 2020). These findings propose the modified biochars, as potentially effective and low-cost remediation technology for polluted soils. However, it should be noted that bioavailability alone may not fully represent the interactions of complex mechanisms involved in

450 soil. Therefore, metals fractionation analysis may offer deeper insights to depict the heavy metals
451 immobilization mechanisms in contaminated soils.

452 Our previous results confirm the efficacy of modified biochars in effectively reducing Cd and Pb leaching
453 by decreasing the availability during the experiments. To further investigate the impact of biochar
454 treatments on Cd and Pb speciation, a sequential extraction procedure was conducted on soil samples after
455 the leaching experiment. The results showed that Cd was dominantly associated with carbonate or oxide
456 or organic bound form (Figure 5). After treatments, specifically Fe-WSBC transformed the exchangeable
457 fraction of Cd and Pb to least available forms, presenting values of 40.91, 36.32%; 15.99, 16.28%; 19.30,
458 15.08%; 17.71, 11.86%; 6.07, 20.44% for exchangeable, carbonate bound, oxide bound, organic matter
459 bound and residual, respectively. Modified biochars effectively transformed Cd and Pb into least
460 available form, enhancing their immobilization in soil and thereby reducing their availability for leaching
461 (Komonweeraket et al., 2015; Mohamed et al., 2015). Overall, it can be inferred that Fe-WSBC and Mg-
462 WSBC effectively immobilized the Cd and Pb in soil as depicted in Figure 6 which can also be further
463 investigated through long-term experiments.

464

465 **4. Conclusion**

466 Here we reported a one-step technology to fabricate wheat straw-derived biochar (Fe-WSBC and Mg-
467 WSBC) which showed superb Cd and Pb adsorption and immobilization in contaminated water (e.g.
468 kinetic, adsorption selectivity, adsorption capacity, pH, real river water) and soil matrices (e.g.
469 availability, immobilization, speciation). The introduction of functional materials demonstrated their
470 efficiency in enhancement of functional moieties on biochar surface, as confirmed by SEM analysis and
471 EDS images, revealing elevated Fe and Mg contents (24.37 and 30.10%) in Fe-WSBC and Mg-WSBC,
472 respectively. The high applicability of prepared adsorbents was verified owing to higher Cd and Pb
473 removal efficiency by employing water experiments. Moreover, Fe-WSBC and Mg-WSBC under flow-

474 through conditions with the application of acidic water had excellent results in reducing Cd and Pb
475 leaching in co-contaminated soil. In addition, various characterization techniques including FTIR, XRD,
476 ad XPS have verified mechanisms involved in understanding the environmental fate of heavy metals and
477 the practical application/utilization of prepared adsorbents. Overall, this study not only offers the
478 viewpoints about the mobility or accumulation of Cd and Pb in water/soil-food system but also highlights
479 the development and application of single material for simultaneous remediation of contaminated water
480 and soil matrices.

481

482 **Acknowledgements**

483 **Data availability**

484 Data will be made available on reasonable request.

485 **Declaration of competing interest**

486 The authors declare they have no known competing financial interests or personal relationships that could
487 influence the work reported in this paper.

488 **References**

489 Boni, M. R., Chiavola, A., Marzeddu, S., 2020. Remediation of Lead-Contaminated Water by Virgin
490 Coniferous Wood Biochar Adsorbent: Batch and Column Application. Water Air Soil Pollut. 231, 171.

491 Boparai, H.K., Joseph, M., O'Carroll, D.M., 2011. Kinetics and thermodynamics of cadmium ion removal
492 by adsorption onto Nano zerovalent iron particles. J. Hazard. Mater. 186, 458–465.

493 Cai, T., Du, H., Liu, X., Tie, B., Zhaoxia Zeng, Z., 2021. Insights into the removal of Cd and Pb from
494 aqueous solutions by NaOH–EtOH-modified biochar. Environmen. Technol. Innovat. 24, 102031.

Cao, Y., Xiao, W., Shen, G., et al., 2019. Carbonization and ball milling on the enhancement of Pb(II) adsorption by wheat straw: Competitive effects of ion exchange and precipitation. Bioresour. Technol. 273, 70–76.

Chen, H., Wang, H., Cui, L., Liu, J., Fan, X., 2022. Comparison of the effects of Fe and Mg modified biochars on the removal of Cd and Pb from contaminated soils. Environ. Sci. .Pollut. Res. 29, 7079-7090.

Chen, K., He, J.Y., Li, Y.L., et al., 2017. Removal of cadmium and lead ions from water by sulfonated magnetic nanoparticle adsorbents. J. Colloid Interface Sci. 494, 307–316.

Deng, Y., Li, X., Ni, F., Liu, Q., Yang, Y., Wang, M., Ao, T., Chen, W., 2021. Synthesis of Magnesium Modified Biochar for Removing Copper, Lead and Cadmium in Single and Binary Systems from Aqueous Solutions: Adsorption Mechanism. Water 13, 599. https://doi.org/10.3390/ w13050599

Dong, J., Shen, L., Shan, S., Liu, W., Qi, Z., Liu, C., Gao, X., 2022. Optimizing magnetic functionalization conditions for efficient preparation of magnetic biochar and adsorption of Pb(II) from aqueous solution. Sci. Total Environ. 806, 151442.

Eom, T.Y., Cho, M., Song, K.Y., Suh, S.J., Park, J.S., Lee, H.J., 2022. Novel Co(OH)F/Zn (OH)F heterostructures for acetone gas sensor applications: Materials synthesis, characterization, and sensor performance evaluation. Sens. Actuators B Chem. 356, 131377.

Fahmi, A. H., Samsuri, A. W., Jol, H., Singh, D., 2018 Bioavailability and leaching of Cd and Pb from contaminated soil amended with different sizes of biochar. R. Soc. Open Sci. 5, 181328. http://dx.doi.org/10.1098/rsos.181328

Gao, R.L., Fu, Q.L., Hu, H.Q., Wang, Q., Liu, Y., Zhu, J., 2019. Highly-effective removal of Pb by co-pyrolysis biochar derived from rape straw and orthophosphate. J. Hazard Mater. 371, 191–197.

Godlewska, P., Bogusz, A., Dobrzyn´ska, J., Dobrowolski, R., Oleszczuk, P., 2020. Engineered biochar modified with iron as a new adsorbent for treatment of water contaminated by selenium. J. Saudi Chem. Soc. 24, 824–834.

Gong, H., Chi, J., 2022. Contribution of different mechanisms to Pb^{2+} and Cd^{2+} sorption on magnetic wheat straw biochars: Impact of pyrolysis temperature and DOM in biochar. J. Environmen. Chem. Eng. 10, 107851.

Habte, L., Shiferaw, N., Thriveni, T., Mulatu, D., Lee, M.-H., Jung, S.-H., Ahn, J.W., 2020. Removal of Cd(II) and Pb(II) from wastewater via carbonation of aqueous $Ca(OH)_2$ derived from eggshell. Process. Saf. Environ. Prot. 141, 278–287, https://doi. org/10.1016/j.psep.2020.05.036.

Hafeez, A., Pan, T., Tian, J., Cai, K., 2022. Modified Biochars and Their Effects on Soil Quality: A Review. Environments 9, 60. https:// doi.org/10.3390/ environments9050060

Hamid, Y., Liu, L., Usman, M., Naidu, R., Haris, M., Lin, Q., Ulhassan, Z., Hussain, M. I., Yang, X., 2022. Functionalized biochars: Synthesis, characterization, and applications for removing trace elements from water. J. Hazard. Mat. 437, 129337.

Hamid, Y., Tang, L., Hussain, B., Usman, M., Liu, L., Cao, X., Ulhassan, Z., Khan, M. B., Yang, X., 2020. Cadmium mobility in three contaminated soils amended with different additives as evaluated by dynamic flow-through experiments. Chemosphere 261, 127763.

Haris, M., Amjad, Z., Usman, M., Saleem, A., Dyussenova, A., Mahmood, Z., Dina, K., Guo, J., Wang, W., 2024. A review of crop residue-based biochar as an efficient adsorbent to remove trace elements from aquatic systems. Biochar, 6:47.

Haris, M., Hamid, Y., Usman, M., Wang, L., Saleem, A., Su, F., Guo, J., Li, Y., 2021. Crop-residues derived biochar: Synthesis, properties, characterization and application for the removal of trace elements in soils. J. Hazard. Mat. 416, 126212.

Haris, M., Usman, M., Saleem, A., Mahmood, Z., Hamid, Y., Guo., J., Xue, S., 2023. Synthesis of conch-like layered carbon nanosheets by ball-milling assisted ultrasonic exfoliation for highly selective removal of Cd(II) from multiple water matrices. Separat. Purific. Technol. 124756.

Haris, M., Usman, M., Su, F., Lei, W., Saleem, A., Hamid, Y., Guo, J., Li, Y., 2022. Programmable synthesis of exfoliated biochar nanosheets for selective and highly efficient adsorption of thallium. Chem. Eng. J. 134842.

Huang, F., Zhang, S.M., Wu, R. R., Zhang, L., Wang, P., Xiao, R. B., 2021. Magnetic biochars have lower adsorption but higher separation effectiveness for Cd^{2+} from aqueous solution compared to nonmagnetic biochars. Environ. Pollut. 275, 116485.

Jia, Y., Zhang, Y., Fu, J., Yuan, L., Li, Z., Liu, C., et al., 2019. A novel magnetic biochar/MgFelayered double hydroxides composite removing Pb^{2+} from aqueous solution: isotherms, kinetics and thermodynamics. Colloids Surf. A Physicochem. Eng. Asp. 567, 278–287.

Jin, H., Hanif, M.U., Capareda, S., et al., 2016. Copper(II) removal potential from aqueous solution by pyrolysis biochar derived from anaerobically digested algae-dairy-manure and effect of KOH activation. J. Environ. Chem. Eng. 4, 365–372.

Kang, X., Geng, N., Li, Y., Li, X., Yu, J., Gao, S., Wang, H., Pan, H., Yang, Q., Zhug, Y., Lou, Y., 2022. Treatment of cadmium and zinc-contaminated water systems using modified biochar: Contaminant uptake, adsorption ability, and mechanism. Bioresour. Technol. 363, 127817.

Karunanayake, A. G., Todd, O. A., Crowley, M. L., Ricchetti, L. B., Pittman Jr., C. U., Anderson, R., Mlsna, T. E., 2017. Rapid removal of salicylic acid, 4-nitroaniline, benzoic acid and phthalic acid from wastewater using magnetized fast pyrolysis biochar from waste Douglas fir. Chem. Eng. J. 319, 75–88.

Ke, Y., Cui, S., Fu, Q., Hough, R., Zhang, Z., Li, Y.F., 2022. Effects of pyrolysis temperature and aging treatment on the adsorption of Cd^{2+} and Zn^{2+} by coffee grounds biochar. Chemosphere 296, 134051.

562 Komonweeraket, K., Cetin, B., Benson, C.H., Aydilek, A.H., Edil, T.B., 2015. Leaching characteristics of
563 toxic constituents from coal fly ash mixed soils under the influence of pH. Waste Manag. 38, 174-184.

564 Kristianto, H., Arie, A. A., Susanti, R. F., Halim, M., Lee, J. K., 2016. The effect of activated carbon
565 support surface modification on characteristics of carbon nanospheres prepared by deposition
566 precipitation of Fe-catalyst, IOP Conf. Ser. Mater. Sci. Eng. 162, 012034.

567 Lei, S., Shi, Y., Qiu, Y., Che, L., Xue, C., 2019. Performance and mechanisms of emerging animal-
568 derived biochars for immobilization of heavy metals. Sci. Total Environ. 646, 1281–1289.

569 Li, A., Ge, W., Liu, L., Zhang, Y., Qiu, G., 2022. Synthesis and application of amine-functionalized
570 MgFe2O4-biochar for the adsorption and immobilization of Cd(II) and Pb(II). Chem. Eng. J. 439,
571 135785.

572 Li, B., Yang, L., Wang, C., Zhang, Q., Liu, Q., Li, Y., Xiao, R., 2017. Adsorption of Cd(II) from aqueous
573 solutions by rape straw biochar derived from different modification processes, Chemosphere 175, 332–
574 340.

575 Li, C., Yi, X., Dang, Z., Yu, H., Zeng, T., Wei, C., & Feng, C., 2016. Fate of Fe and Cd upon microbial
576 reduction of Cd-loaded polyferric focs by Shewanella oneidensis MR-1. Chemosphere, 144, 2065–2072.

577 Li, H., Li, X., Li, W., Li, J., Li, Y., Wu, J., 2021a. Immobilization of heavy metals in contaminated soil
578 using Fe-modified biochar. Chemosphere, 278, 130440.

579 Liu, X., Yang, L., Zhao, H., Wang, W., 2020. Pyrolytic production of zerovalent iron nanoparticles
580 supported on rice husk-derived biochar: simple, in situ synthesis and use for remediation of Cr(VI)-
581 polluted soils. Sci. Total Environ. 708, 134479.

582 Lun, M. K., Lin, H., He, Y. H., Li, B., Dong, Y. B., Wang, L., 2019. Efficient simultaneous removal of
583 cadmium and arsenic in aqueous solution by titanium-modified ultrasonic biochar. Bioresour. Technol.
584 284, 333–339.

585 Luo, H., Lin, Q., Zhang, X., et al., 2019. New insights into the formation and transformation of active
586 species in nZVI/BC activated persulfate in alkaline solutions. Chem. Eng. J. 359, 1215–1223.
587 http://dx.doi.org/10.1016/j.cej.2018.11.056.

588 Ma, Y., Wu, L.,P. Li, P., Yang, L., He, L., Chen, S., Yang, Y., Gao, F., Qi, X., Zhang, Z., 2021. A novel,
589 efficient and sustainable magnetic sludge biochar modified by graphene oxide for environmental
590 concentration imidacloprid removal, J. Hazard. Mater. 407, 124777,
591 https://doi.org/10.1016/j.jhazmat.2020.124777.

592 Miao, Q., Li, G., 2021. Potassium phosphate/magnesium oxide modified biochars: Interfacial chemical
593 behaviours and Pb binding performance. Sci. Total Environ. 759, 143452.

594 Mohamed, I., Zhang, G., Li, Z., Liu, Y., Chen, F., Dai, K., 2015. Ecological restoration of an acidic Cd
595 contaminated soil using bamboo biochar application. Ecol. Eng. 84, 67-76.

596 Naeem, M. A., Imran, M., Amjad, M., Abbas, G., Tahir, M., Murtaza, B., Zakir, A., Shahid, M., Bulgariu,
597 L., Ahmad, I., 2019. Batch and Column Scale Removal of Cadmium from Water Using Raw and Acid
598 Activated Wheat Straw Biochar. Water 11, 1438.

599 Ni, B.-J., Huang, Q.-S., Wang, C., Ni, T.-Y., Sun, J., Wei, W., 2019. Competitive adsorption of heavy
600 metals in aqueous solution onto biochar derived from anaerobically digested sludge, Chemosphere 219,
601 351–357.

602 Novak, J. M., Busscher, W. J., Watts, D. W., Laird, D. A., Ahmedna, M.A., Niandou, M.A.S., 2010.
603 Short-term CO_2 mineralization after additions of biochar and switchgrass to a Typic Kandiudult.
604 Geoderma 154, 281-288.

Page, K., Harbottle, M. J., Cleall, P. J., Hutchings, T. R., 2014. Heavy metal leaching and environmental risk from the use of compost-like output as an energy crop growth substrate. Sci. Total Environ. 487, 260–271.

Ren, J., Yu, P., Xu, X., 2019. Straw Utilization in China—Status and Recommendations. Sustainability 11, 1762.

Sackey, E. A., Song, Y., Yu, Y., Zhuang, H., 2021. Biochars derived from bamboo and rice straw for sorption of basic red dyes. PLoS ONE 16, e0254637.

Sha, H., Li, J., Wang, L., Nong, H., Wang, G., Zeng, T., 2023. Preparation of phosphorus modified biochar for the immobilization of heavy metals in typical lead-zinc contaminated mining soil: Performance, mechanism and microbial community. Environ. Res. 218, 114769.

Shaheen, S. M,, Natasha, A., Mosa, A., El-Naggar, A., Hussain, M, F., Abdelrahman, H., Niazi, N. K., Shahid, M., Zhang, T., Tsang, Y. F., Trakal, L., Wang, S., Rinklebe, J., 2022a. Manganese oxide-modified biochar: production, characterization and applications for the removal of pollutants from aqueous environments—a review. Bioresour. Technol. 346, 126581.

Shaheen, S. M., Antoniadis, V., Shahid, M., Yang, Y., 2022b. Sustainable applications of rice feedstock in agro environmental and construction sectors: a global perspective. Renew. Sustain. Energy. Rev. 153, 111791.

Shi, Q., Zhang, H., Shahab, A., Zeng, H., Zeng, H., Bacha, A. U. R., Nabi, I., Siddique, J., Ullah, H., 2021. Efficient performance of magnesium oxide loaded biochar for the significant removal of Pb^{2+} and Cd^{2+} from aqueous solution. Ecotoxicol. Environ. Saf. 221, 112426.

Song, J., Messele, S.A., Meng, L., Huang, Z., Gamal El-Din, M.G., 2021. Adsorption of metals from oil sands process water (OSPW) under natural pH by sludge based Biochar/chitosan composite. Water Res. 194, 116930. https://doi.org/10.1016/j. watres.2021.116930.

628 Tan, Y., Yin, X.Q., Wang, C.Y., Sun, H.M., Ma, A.S., Zhang, G.L., Wang, N., 2019. Sorption of
629 cadmium onto Mg-Fe Layered Double Hydroxide (LDH)-Kiwi branch biochar. Environ. Pollut.
630 Bioavailab. 31, 189–197.

631 Tang, J.Y., Zhang, L.H., Zhang, J.C., et al., 2020. Physicochemical features, metal availability and
632 enzyme activity in heavy metal-polluted soil remediated by biochar and compost. Sci. Total Environ. 701,
633 134751.

634 Tao, Q., Li, B., Li, Q., Han, X., Jiang, Y., Jupa, R., Wang, C., Li, T., 2019. Simultaneous remediation of
635 sediments contaminated with sulfamethoxazole and cadmium using magnesium-modified biochar derived
636 from Thalia dealbata. Sci. Total Environ. 659, 1448–1456.

637 Tehrani, M.M., Abbasizadeh, S., Alamdari, A., Mousavi, S.E., 2017. Prediction of simultaneous sorption
638 of copper(II). Desalin. Water Treat. 62, 403–417. https://doi. org/10.5004/dwt.2017.20135.

639 Tie, J., Li, W., Liu, H., Huang, K., Mi, X., Wei, M., Hou, L., 2023. Efficient adsorption and reduction of
640 Cr(VI) by a novel polyaniline modified magnetic iron-based waterworks sludge from aqueous solution.
641 Chem. Eng. J. 451, 137673.

642 Tumampos, S. B., Ensano, B. M. B., Pingul-Ong, S. M. B., Ong, D. C.,. Kan, C. C., Yee, J. J., de Luna,
643 M. D. G., 2021. Isotherm, Kinetics and Thermodynamics of Cu (II) and Pb (II) Adsorption on
644 Groundwater Treatment Sludge-Derived Manganese Dioxide for Wastewater Treatment Applications, Int.
645 J. Environ. Res. Publ. Health 18(6). https://doi. Org/10.3390/ijerph18063050.

646 Van Poucke, R., Meers, E., Tack. F. M. G., 2020. Leaching behavior of Cd, Zn and nutrients (K, P, S)
647 from a contaminated soil as affected by amendment with biochar. Chemosphere 245, 125561.

648 Wan, X., Li, C., Parikh, S. J., 2020. Simultaneous removal of arsenic, cadmium, and lead from soil by
649 iron-modified magnetic biochar. Environ. Pollut. 261, 114157.

Wang, Y., Xu, Y., Liang, X., Sun, Y., Huang, Q., Peng, Y., 2019. Leaching behavior and efficiency of cadmium in alkaline soil by adding two novel immobilization materials, Science of the Total Environment, https://doi.org/10.1016/j.scitotenv.2019.13596.

Wang, Y., Zheng, K., Jiao, Z., Zhan, W., Ge, S., Ning, S., Fang, S., Ruan, X., 2022. Simultaneous Removal of Cu2+, Cd2+ and Pb2+ by Modified Wheat Straw Biochar from Aqueous Solution: Preparation, Characterization and Adsorption Mechanism. Toxics 10, 316.

Wang, Z., Zheng, H., Luo, Y., Deng, X., Herbert, S., Xing, B., 2013. Characterization and influence of biochars on nitrous oxide emission from agricultural soil. Environ. Pollut. 174, 289-296.

Wu, J., Huang, D., Liu, X., Meng, J., Tang, C., Xu, J., 2018. Remediation of As(III) and Cd(II) co-contamination and its mechanism in aqueous systems by a novel calcium-based magnetic biochar. J. Hazard. Mat. 348, 10–19.

Xiao, J., Hu, R., Chen, G., 2020. Micro-nano-engineered nitrogenous bone biochar developed with a ball-milling technique for high-efficiency removal of aquatic Cd (II), Cu(II) and Pb(II). J. Hazard. Mater. 387, 121980. https://doi.org/10.1016/j. jhazmat.2019.121980.

Xiao, R., Wang, J. J., Li, R., Park, J., Meng, Y., Zhou, B., Pensky, S., Zhang, Z., 2018. Enhanced sorption of hexavalent chromium [Cr(VI)] from aqueous solutions by diluted sulfuric acid-assisted MgO-coated biochar composite. Chemosphere, 208, 408–416.

Xu, J., Zhang, Y., Li, B., Fan, S., Xu, H., Guan, D-X., 2022. Improved adsorption properties of tetracycline on KOH/KMnO4 modified biochar derived from wheat straw. Chemosphere 296,133981.

Yu, W., Hu, J., Yu, Y., Ma, D., Gong, W., Qiu, H., Hu, Z., Gao, H.-W., 2021. Facile preparation of sulfonated biochar for highly efficient removal of toxic Pb(II) and Cd(II) from wastewater, Sci. Total Environ. 750, 141545, https://doi.org/10.1016/j. scitotenv.2020.141545.

672 Zhang, F., Wang, X., Xionghui, J., Ma, L., 2016. Efficient arsenate removal by magnetitemodified water
673 hyacinth biochar, Environ. Pollut. 216, 575–583.

674 Zhang, J., Hou, D., Shen, Z., Jin, F., O'Connor, D., Pan, S., Ok, Y. S., Tsang, D. C. W., Bolan, N. S.,
675 Alessi, D. S., 2020. Effects of excessive impregnation, magnesium content, and pyrolysis temperature on
676 MgO-coated watermelon rind biochar and its lead removal capacity. Environmen. Res. 183, 109152.

677 Zhang, M., Gao, B., Yao, Y., Xue, Y., Inyang, M., 2012. Synthesis of porous MgO-biochar
678 nanocomposites for removal of phosphate and nitrate from aqueous solutions. Chem. Eng. J. 210, 26-32.

679 Zhao, Y., Zhang, R., Liu, H., Li, M., Chen, T., Chen, D., Zou, X., Frost, R. L., 2019. Green preparation of
680 magnetic biochar for the effective accumulation of Pb (II): Performance and mechanism. Chem. Eng. J.
681 375, 122011.

682 Zheng, Y., Wan, Y., Chen, J., Chen, H., Gao, B., 2020. MgO modified biochar produced through ball
683 milling: A dual-functional adsorbent for removal of different contaminants. Chemosphere 243, 125344.

684 Zhou, Q., Liao, B., Lin, L., Qiu, W., Song, Z., 2018. Adsorption of Cu(II) and Cd(II) from aqueous
685 solutions by ferromanganese binary oxide–biochar composites. Sci. Total Environ. 615, 115–122.

686 Zhou, Y., Liu, X., Tang, L., Zhang, F., Zeng, G., Peng, X., Luo, L., Deng, Y., Pang, Y., Zhang, J., 2017.
687 Insight into highly efficient co-removal of p-nitrophenol and lead by nitrogen-functionalized magnetic
688 ordered mesoporous carbon: Performance and modelling. J. Hazard. Mater. 333, 80–87.

689

Table 1. Isotherm parameters for Cd and Pb adsorption on WSBC, Fe-WSBC and Mg-WSBC

Treatments		Langmuir model			Freundlich model			Temkin model		
		Q_{max} (mg g^{-1})	k_L(L mg^{-1})	R^2	K_F (L g^{-1})	1/n	R^2	k_T (L g^{-1})	b (KJ mol^{-1})	R^2
Cd	WSBC	34.21	0.0023	0.981	2.668	0.704	0.97	0.079	9.872	0.911
	Fe-WSBC	82.84	0.0044	0.982	9.268	0.3815	0.966	0.3018	16.604	0.899
	Mg-WSBC	65.48	0.0038	0.992	4.601	0.4608	0.959	0.1224	16.50	0.932
Pb	WSBC	48.20	0.389	0.993	50.04	0.510	0.989	0.116	11.82	0.911
	Fe-WSBC	111.24	0.5317	0.991	41.91	0.613	0.979	0.28	23.09	0.931
	Mg-WSBC	88.64	0.0372	0.99	46.21	0.613	0.986	0.18	20.9	0.948

Table 2: Comparison of the adsorption capacities of Fe-WSBC and Mg-WSBC with other Fe and Mg modified biochars for Cd and Pb removal from aqueous solution

Adsorbent	Target element	Dosage	Solution pH	Adsorption capacity	R^2 value	References
Amine-functionalized $MgFe_2O_4$-biochar	Cd, Pb	0.05 g	----	200 and 200 mg g^{-1}	Langmuir: 0.987 and 0.985	Li, A et al., 2022
Magnetic wheat straw biochar	Cd, Pb	3 g	5.0 ± 0.1	7.50–31.68 and 151.6–298.2 mg g^{-1}	----	Gong and Chi, 2022
Wheat straw magnetic biochar	Pb	0.1 g	5.0 ± 0.1	18.86-196.91 mg g^{-1}	Langmuir: 0.930	Zhao et al., 2019
Rice straw magnetic biochar	Cd	1 g	6.0	30.23 mg g^{-1}	Langmuir: 0.9709	Huang et al., 2021
Sewage sludge magnetic biochar	Cd	1 g	6.0	2.61 mg g^{-1}	Freundlich: 0.9833	Huang et al., 2021
Calcium-based magnetic biochar (Rice straw)	Cd	50 mg	7.0	10.07 mg g^{-1}	Langmuir: 0.923	Wu et al., 2018
Magnesium oxide loaded-eucalyptus biochar	Cd, Pb	0.02 g	5.0	515.17 and 829.11 mg g^{-1}	Langmuir: 0.966 and 0.873	Shi et al., 2021
$MgCl_2$ modified biochar	Cd	0.5 g	7.0	Sorption increased by 24.2–25.6%	Langmuir: > 0.944	Tao et al., 2019
Wheat straw biochar modified by phosphate/magnesium	Pb	30 mg	5.0 ± 0.1	308.39 mg g^{-1}	Langmuir: 0.999	Miao and Li, 2021

MgO-coated watermelon rind biochar	Pb	0.1 g	----	558 mg g^{-1}	----	Zhang et al., 2020
Fe-modified wheat straw biochar (Fe-WSBC)	Cd, Pb	0.02 g	6 ± 0.5	82.8 and 111.24 mg g^{-1}	Langmuir: 0.982, 0.991	This study
Mg-modified wheat straw biochar (Mg-WSBC)	Cd, Pb	0.02 g	6 ± 0.5	65.4 and 88.64 mg g^{-1}	Langmuir: 0.992, 0.990	This study

Figure 1: Adsorption kinetics of Cd and Pb (PFO and PSO) (a,b), IPD model (c,d), and isotherm models (e,f)

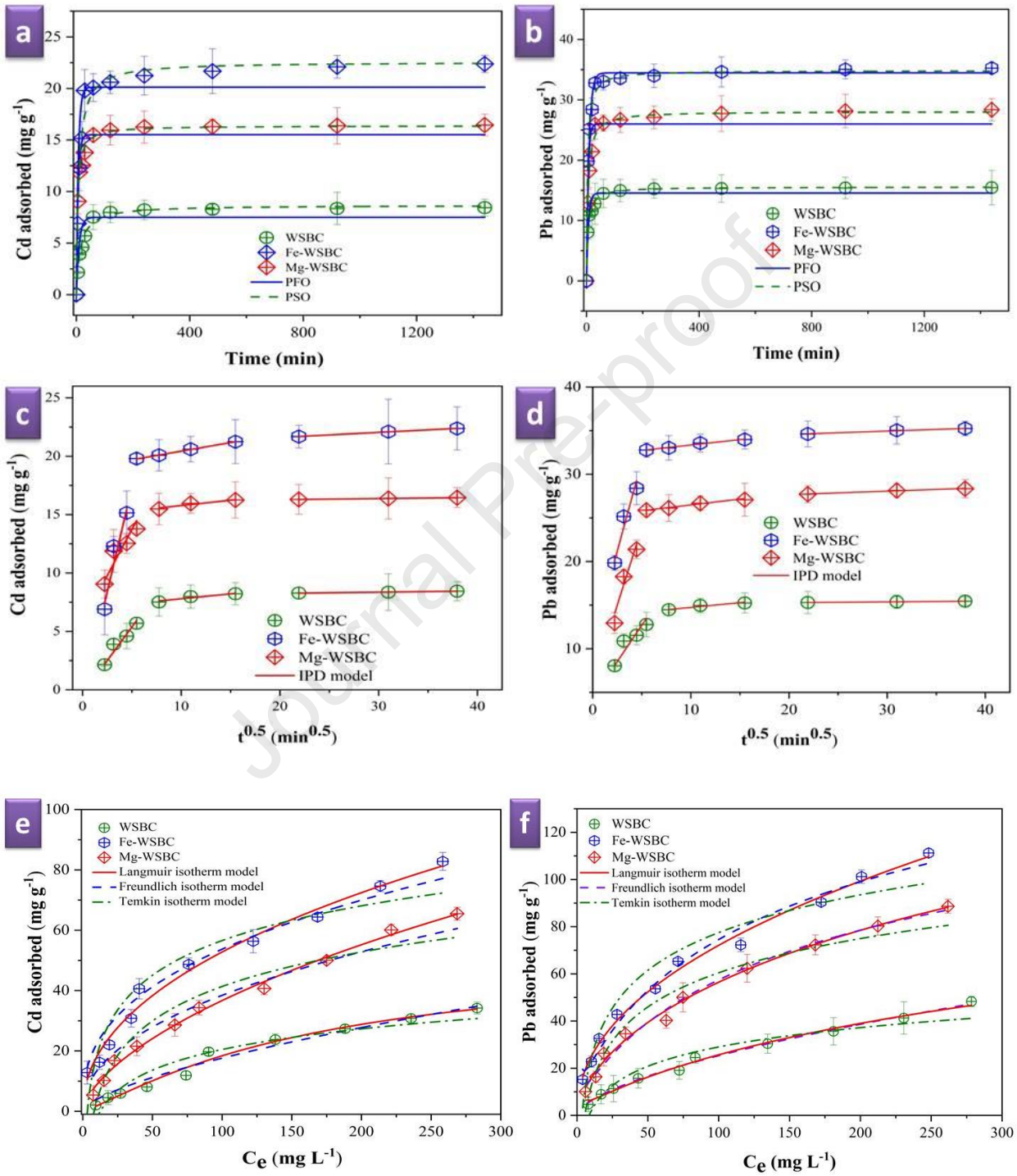

Figure 2: FTIR (a,b) and XRD (c) analysis after Cd and Pb adsorption from contaminated solution

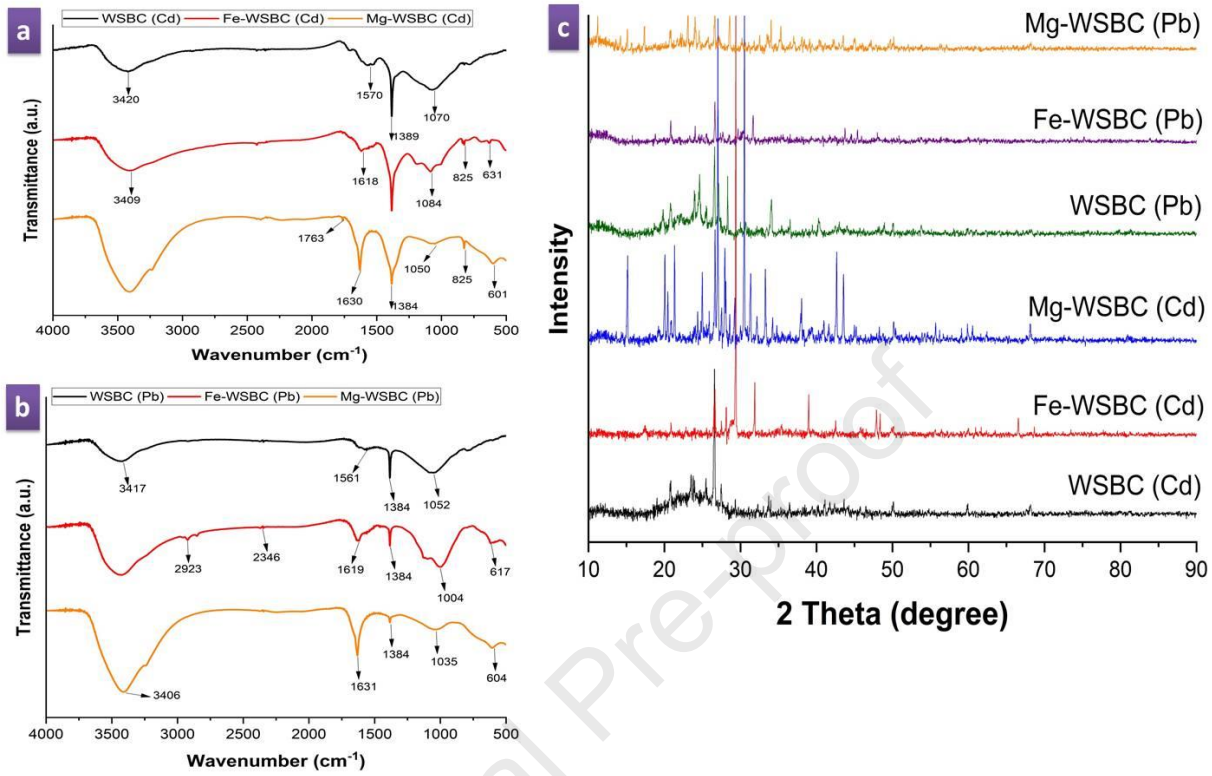

Figure 3: Effect of amendments on Cd and Pb removal from spiked river water (a,b) and Reusability of WSBC, Fe-WSBC, and Mg-WSBC (c,d)

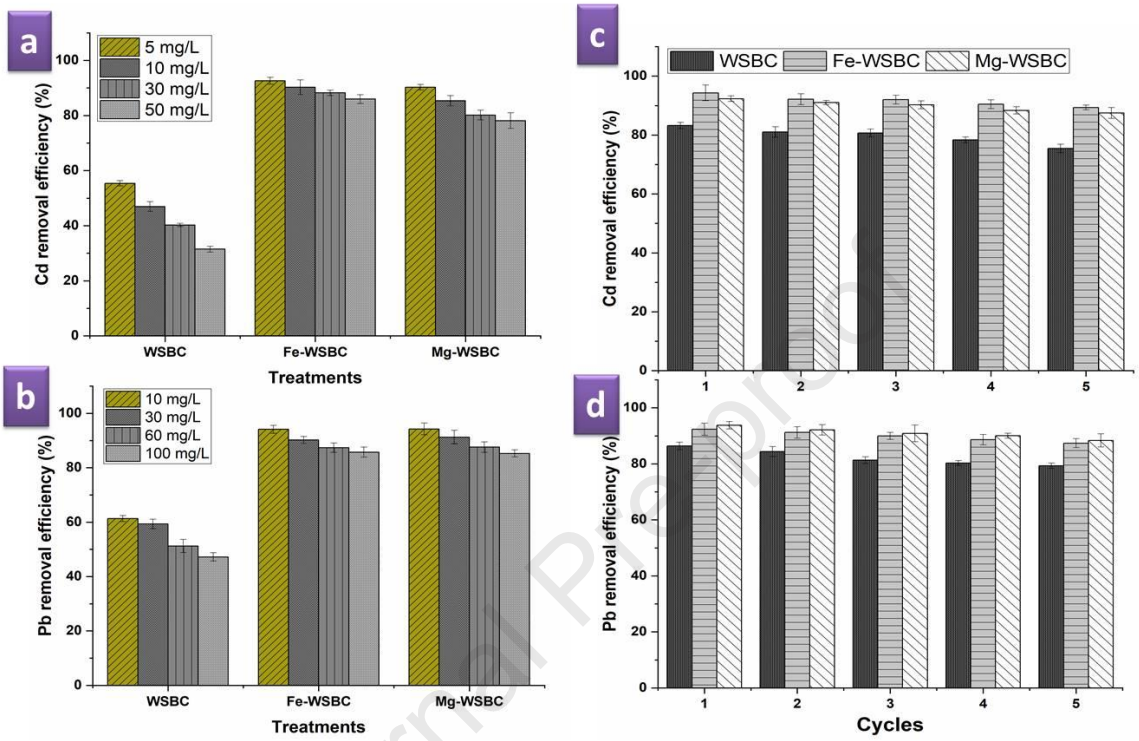

Figure 4: Effect of WSBC, Fe-WSBC, and Mg-WSBC on Cd and Pb concentration in leachate collected from leaching experiment

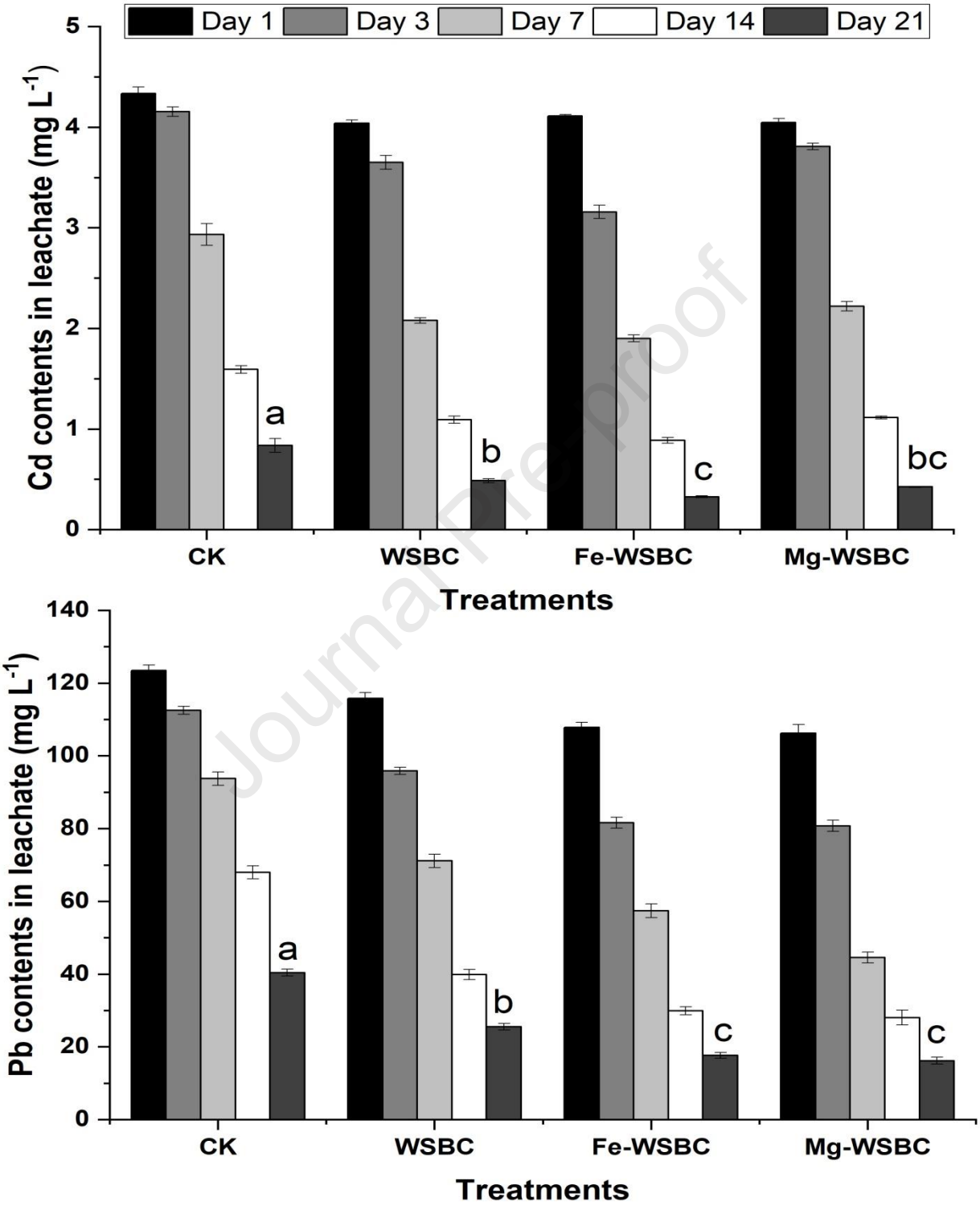

Figure 5: Effect of WSBC, Fe-WSBC, and Mg-WSBC on Cd and Pb available contents and speciation in soil after leaching experiment

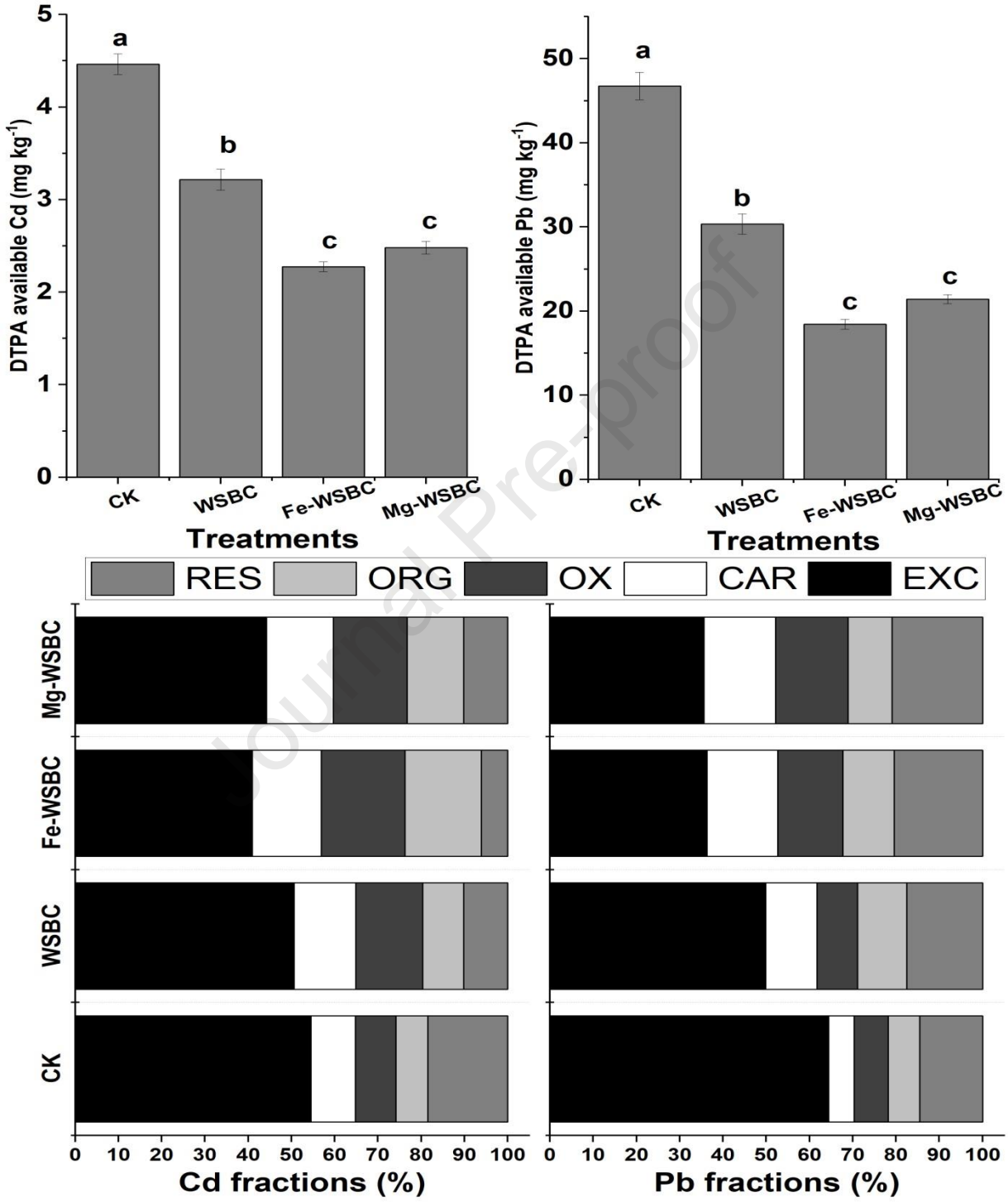

Figure 6: Characterization and mechanistic approaches of WSBC, Fe-WSBC and Mg-WSBC to understand the mechanism involved in HMs abatement in contaminated matrices

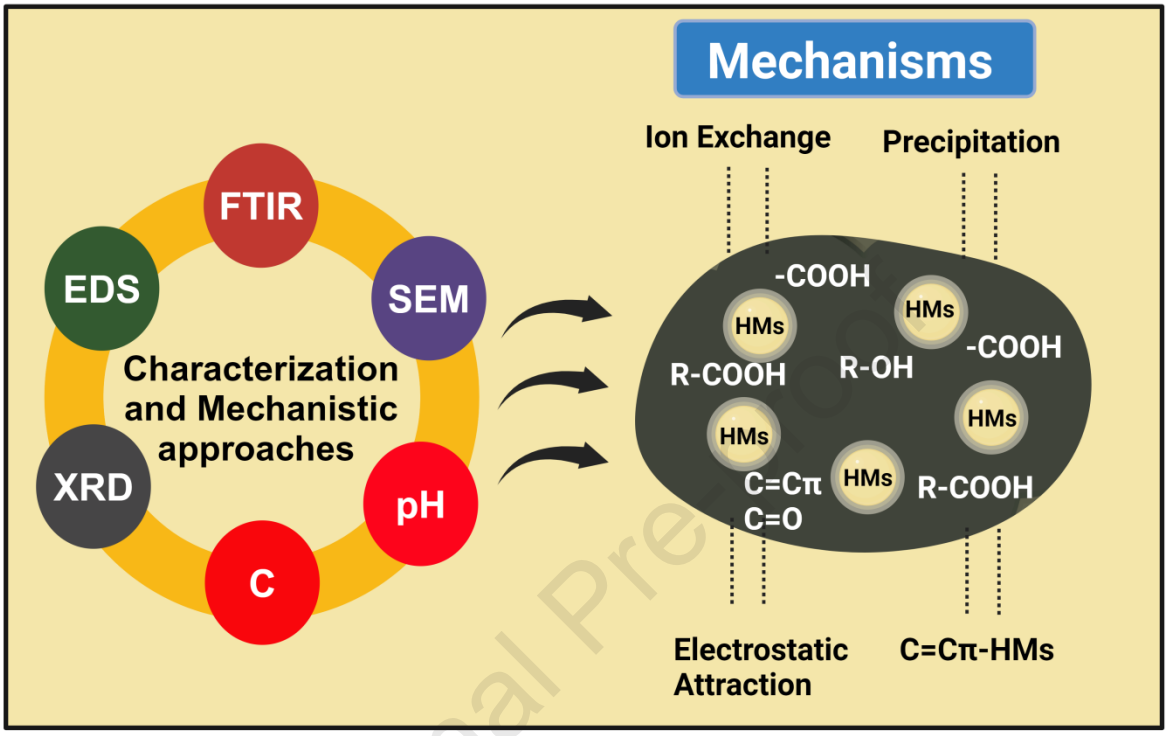

Highlights

- The functionalized biochars were deployed under batch adsorption and leaching trial
- Fe-WSBC adsorbed higher Cd and Pb (82.84 and 111.24 mg g^{-1}) than Mg-WSBC and WSBC
- The leachability of Cd and Pb was reduced to 0.326 and 17.62 mg L^{-1} with Fe-WSBC
- Fe-WSBC altered the metals' exchangeable form to residual form, lowering the leaching

Declaration of interests

☐ ✓ The authors declare that they have no known competing financial interests or personal relationships that could have appeared to influence the work reported in this paper.

☐ The authors declare the following financial interests/personal relationships which may be considered as potential competing interests:

The authors declare they have no known competing financial interests or personal relationships that could influence the work reported in this paper